analytical chemistry

Article

pubs.acs.org/ac

Impedimetric Detection of Pathogenic Gram-Positive Bacteria Using an Antimicrobial Peptide from Class IIa Bacteriocins

Hashem Etayash,[†,‡] Keren Jiang,[‡] Thomas Thundat,[‡] and Kamaljit Kaur*[,†]

[†]Faculty of Pharmacy and Pharmaceutical Sciences, University of Alberta, Edmonton, Alberta, T6G 2E1, Canada

[‡]Department of Chemical and Materials Engineering, University of Alberta, Edmonton, Alberta, T6G 2V4, Canada

Supporting Information

ABSTRACT: Real-time, label-free detection of Gram-positive bacteria with high selectivity and sensitivity is demonstrated using an interdigitated impedimetric array functionalized with naturally produced antimicrobial peptide from class IIa bacteriocins. The antimicrobial peptide, leucocin A, was chemically synthesized and covalently immobilized on interdigitated gold microelectrodes via the interaction between the C-terminal carboxylic acid of the peptide and free amines of a preattached thiolated linker. Exposing the peptide sensor to various concentrations of Gram-positive bacteria generated reproducible impedance spectra that detected peptide−bacteria interactions at a concentration of 1 cell/μL. The peptide sensor also selectively detected *Listeria monocytogenes* from other Gram-positive strains at a concentration of 10^3 cfu mL^{-1}. The study highlights that short peptide ligands from bacteriocin class offer high selectivity in bacterial detection and can be used in developing a robust, portable biosensor device to efficiently detect pathogenic Gram-positive bacteria in food samples.

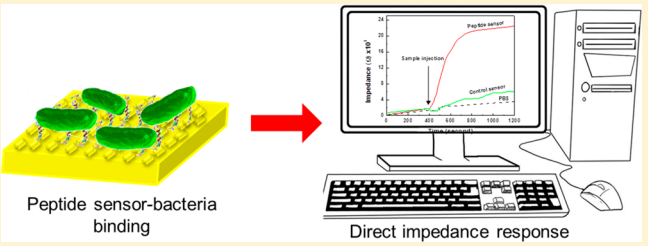

Food contaminations and emergence of resistant bacteria remain as the critical concerns in developed and developing nations due to the lack of hand-held or portable devices for fast detection of pathogenic bacteria with high sensitivity and selectivity.[1,2] For nearly a century, the conventional approaches for bacterial testing have relied and "continue to rely" almost exclusively on specific microbiologic media to segregate and enumerate the existing viable bacterial cells.[3] The steps involved in these detection techniques are labor-intensive, time-consuming, and require trained personal in a laboratory setting. Therefore, conventional methods are inadequate for making timely assessments on microbiological safety of food and pharmaceutical products. Over the years, many biological procedures have been simplified and faster methods for detection with significantly reduced assay time and enhanced sensitivity have been developed.[4] Most importantly, these advanced biotechnological assays, referred to as "rapid detection techniques" have spawned a new generation of analytical methods that no longer rely exclusively on agar media.[5,6] These techniques encompass a large and diverse group of systems and devices including miniaturized biochemical assays,[3] physicochemical tests based on bacterial metabolites, antibody−antigen interactions,[7,8] DNA- and enzyme-based tools,[6,9−11] and even fully automated diagnostic systems. The majority of these advanced detection approaches rely on antibody and nucleic acid probes for recognition, identification, and quantification of the target bacterial cells. These techniques include immunoassays[8] and polymerase chain reaction (PCR),[5] as well as biosensor-based platforms with immobilized receptors.[12−14]

Immunoassays for detecting bacteria typically use monoclonal antibodies (Mab) that recognize the antigens unique to specific bacteria. In this method, microplate wells precoated with polyclonal antibodies to bacteria are used to capture antigens from the test samples. Subsequently, the antigens are detected with horseradish peroxidase-labeled Mab followed by reaction with a chromogenic substrate.[7] PCR-based methods require extraction of DNA by rupturing the cells followed by precipitation of nucleic acids. DNA is then amplified by PCR, and unique DNA sequences such as 16SrDNA are analyzed as target genes for specific detection of bacteria. These techniques are widely accepted and used as standard protocols for detection and quantification of numerous foodborne and waterborne pathogenic bacteria.

Despite the fact that these methods are very powerful and versatile tools for detecting, monitoring, and clinical diagnosis of pathogen infections with specificity and sensitivity, they still suffer from a number of constraints that limit their widespread applications. Antibody-based platforms, for instance, lack ample stability at harsh environmental conditions, and there is a high cost of monoclonal antibody developments and the need for a well-trained microbiologist to perform the tests.[15] Similarly, nucleic acid probes based techniques are very costly, labor-intensive, and require pretreatments to extract the DNA.[11] In contrast to antibody and DNA probes, antimicrobial peptides (AMPs) are intrinsically more stable in harsh environments,

Received: October 28, 2013
Accepted: January 8, 2014
Published: January 8, 2014

easier to synthesize, and exhibit broad activities and affinities against wide range of Gram-positive and Gram-negative strains of bacteria.[16]

Several recent studies have explored the viability of using the AMPs as molecular recognition elements in biosensor platforms and have demonstrated the ability of naturally occurring AMPs to serve as robust biorecognition probes in electronic biosensors.[17−21] For example, Mannoor et al. reported the use of gold microelectrodes with AMP magainin I immobilized from the C-terminal cysteine residue to detect pathogenic strains of *Escherichia coli* and *Salmonella*.[18] They also showed that antimicrobial peptides self-assembling onto a wireless graphene nanosensor can be used for bioselective detection of bacteria at single-cell levels.[22] We recently showed that surface-anchored peptide segment of a class IIa bacteriocin is able to bind selectively only to Gram-positive bacteria.[23] Although AMP-based platforms are gaining popularity, some limitations remain to be worked out before this technology becomes widely used. Methods for peptide immobilization to deliver constant peptide density over different surfaces and false positive signal from nonspecific binding of other biomolecules present in test samples such as milk, ready-to-eat meat, and pharmaceutical products, remain as key challenges in this field.

Here we report on utilizing the antimicrobial peptides as selective probes for label-free, real-time detection of foodborne pathogens using a new generation of impedance array analyzer that works at very low frequencies. We have functionalized the arrays with an antilisterial antimicrobial peptide from class IIa bacteriocins for selectivity.[24] The functionalized electrode array is a promising sensor platform to be analyzed using impedance spectroscopy due to its simplicity, high sensitivity, miniature size, ease of assembly, and flexibility for multiplexed lab-on-a-chip applications.[21,25] It has lately been proven to be a very effectual tool for studies including detection of DNA hybridization,[25] antigen−antibody interactions, and most recently in detection of cancer biomarkers.[26,27] Leucocin A (LeuA) is a well-known, naturally occurring AMP from class IIa bacteriocins.[28,29] It consists of 37 amino acid residues, and similar to other class IIa bacteriocins, it is characterized by a conserved disulfide bond and a YGNGV sequence near the N-terminus and a C-terminal domain with an amphiphilic α-helix ending with a hairpin-like structure at the C-terminal tail.[29] Unlike most AMPs that are usually broad spectrum and act via nonspecific mechanisms, class IIa bacteriocins possess narrow activity spectrum with high potency (typically active in the nanomolar range) and act by receptor-mediated mechanism on the target bacterial cells. Class IIa bacteriocins exhibit high potency against various strains of Gram-positive *Listeria monocytogenes* and are therefore also known as antilisterial antimicrobial peptides.[23,24] LeuA, a representative class IIa bacteriocin, exhibits activity against Listeria in the nanomolar range with a minimum inhibitory concentration (MIC) of ∼37 nM.[30] These peptides achieve such potent activity most likely by specific binding interaction with membrane-located proteins of the mannose phosphotransferase system (man-PTS).[31−33] Different expression levels of the mannose receptor on surface of the bacterial cells, from one to another strain, lead to various sensitivities and activities of bacteriocins.[33] An antimicrobial peptide from class IIa bacteriocins immobilized on electrode arrays for impedance spectroscopy offers an ideal sensor platform for real-time detection of *L. monocytogenes* in solutions. We used the multiplexing capabilities of our custom-designed antimicrobial peptide impedance microelectrodes (Figure 1) for demonstrating the detection of different types of foodborne pathogens in contaminated milk samples.

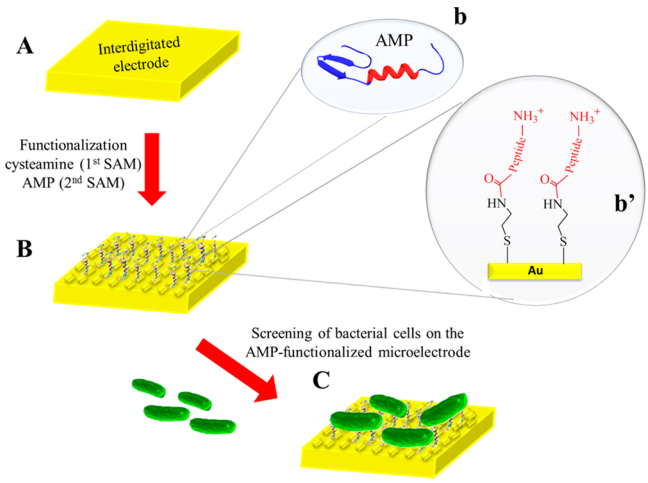

Figure 1. Graphic depiction of the AMP-based biosensor showing (A) a simulated cartoon denoting the interdigitated microelectrode, (B) AMP immobilized on the microelectrode array, and (C) bacterial detection achieved via binding of the target cells to the immobilized AMP. Also shown are (b) the NMR solution structure of the AMP leucocin A[34] and (b′) the chemistry of surface functionalization.

MATERIALS AND METHODS

Antimicrobial Peptide and Cell Culture. Leucocin A is a 37 residue class IIa bacteriocin that contains one disulfide bond between Cys9 and Cys14 in the N-terminal region. LeuA (NH_2−KYYGNGVHCTKSGCSVNWGEAFSAGVHRLA-NGGNGFW−COOH) was chemically synthesized using solid-phase peptide synthesis as described previously.[35] Stocks of bacterial cells, *L. monocytogenes* ATCC 43256 (grown in TSBYE, 37 °C), *Listeria innocua* ATCC 33090 (grown in TSBYE, 37 °C), *Enterococcus faecalis* ATTC 19433 (APT broth, 37 °C), and *Staphylococcus aureus* ATCC 13565 (APT broth, 37 °C), were obtained from CanBiocin Edmonton Inc. All experiments related to the pathogenic bacterial subculture, maintenance, and treatments were carried out in a level II biosafety cabinet.

Impedance Spectroscopy. An impedance spectroscopic analyzer SHARP IA-2 (Sharp Laboratory, U.S.A.) was used to measure impedance response. The instrument is capable of measuring up to 15 channels simultaneously at a fixed frequency in the range of 10−1000 Hz and a stimulation voltage of 10−212 mV. The sensor array consists of 15 interdigitated gold electrodes enclosed in three separate reaction chambers. The individual impedimetric sensor electrode has a typical dimension of 3350 μm × 100 μm × 150 nm, and the spacing between the sensor electrode and the common electrode is 40 μm. The size of each die of fabricated impedimetric microarray was 20 mm × 18.5 mm. The impedance analyzer is also equipped with a sensor for temperature control which was set at 25 °C.

Impedance Array Functionalization. Surface functionalization with antimicrobial peptide was based on covalent interaction between the accessible carboxylic group of the peptide and a free amine group of a thiol linker preattached to the electrode's surface. Figure 1 shows schematic of the sensing platform revealing the immobilization approach. First, the gold

dx.doi.org/10.1021/ac4034938 | *Anal. Chem.* 2014, 86, 1693−1700

interdigitated electrodes were functionalized with a cysteamine linker ($HSCH_2CH_2NH_2$) by treatment with cysteamine hydrochloride (0.01 M) in concentrated buffer solution (8× PBS, pH 8.1) for 6 h.[36] The electrodes were then rinsed with 1× PBS (pH 7.4) to remove any unbound thiol linker. Stock solution of AMP (800 μg/mL) in 1× PBS (pH 7.4) containing EDC (0.2 M) as activating agent was injected into the sensing chambers and incubated overnight at room temperature. The functionalized electrodes were then rigorously washed with 1× PBS to remove any unbound AMP, rinsed with deionized water, and dried in liquid nitrogen.

Impedance Setup and Measurements. The IA-2 analyzer operation is based on electrochemical impedance spectroscopy.[37] When the AMP captures its specific target biomolecules from the surrounding medium, the molecular interactions lead to changes in the sensor's impedance that are correlated to the type and amount of the bound analytes. The changes thereby are detected, measured, and analyzed by monitoring impedimetric parameters. The data presented in this study were performed at 10−120 Hz and 100 mV stimulation signal for bacterial detection in both PBS and milk samples. Initially, to optimize an adequate frequency for the detection, bacterial cells (*L. monocytogenes* and *E. faecalis*) at 10^3 cfu mL^{-1} were exclusively incubated with the peptide sensor arrays and the impedance readings were taken at different frequencies ranging from 10 to 100 Hz. In each study, prior to measurements of the peptide−bacteria interactions, the sensor array fluidic chambers were filled with target-free sample (no bacteria) and subjected to impedance reading for 400 s to establish the baseline. Target-containing sample was then incubated in the sensor chamber and subjected to another impedance reading for ∼800 s.

For sensitivity measurements, pathogenic Gram-positive *L. monocytogenes* at serial concentrations of 10^2, 10^3, 10^4, 10^5, and 10^6 cfu mL^{-1} were individually injected into the sensor array fluidic chambers, incubated with the immobilized peptide, and subjected to impedance reading for ∼800 s at 100 Hz.

Impedance Measurements with Different Bacterial Strains and Contaminated Milk. Selectivity in detection was performed with various bacterial strains (10^3 cfu mL^{-1} each) at a 100 Hz and 25 °C. For the real-time measurements, the impedance versus time data were recorded for the bacterial solutions incubated in the microfluidic channels. All experiments were repeated at least three times. Contaminated milk samples were prepared by mixing milk (100−1000 μL, 2.0% homogenized milk) with PBS (900−0 μL) followed by addition of *L. monocytogenes*, 10^3 cfu mL^{-1}. Milk samples with and without bacteria were then independently incubated in the microfluidic chambers, and impedance reading were recorded at 100 Hz at 25 °C. Finally, the sensor device was regenerated by cleaning the microfluidic chambers (to remove all adhered bacterial cells) with a 70% absolute ethanolic solution, followed by rinsing with DI water and drying under nitrogen.

Data Analysis. Data analysis software is based on a previously described algorithm,[25,38] which is incorporated into the IA-2 instrument user interface. The interaction chemistry suggests that the immobilized antimicrobial peptide captures the target cells (bacteria) at a rate that follows an exponential function. This rate changes with time after introduction of the target cells into the fluidic chamber. Therefore, the binding curve at a fixed frequency is analyzed as an exponentially varying impedance signal Z over time t according to eq 1:[38]

$$|Z(t)| = B + A[1 - \exp(-st)] \quad (1)$$

where s, A, and B are independent constants. B is the offset at which the exponential begins and denotes the array impedance baseline of the target-free buffer solution. Both s and A hold important biochemical parameters. The first is the amplitude of the impedance signal response, and the latter is correlated to the rate of exponential time constant associated with target binding. The algorithm automatically extracts the kinetic parameters from eq 1 and computes the amplitude of impedance response corresponding to the peptide−bacteria interactions. The curve was analyzed as an exponentially varying impedance signal, and the parameters calculations reflect the target concentration, sensor surface coverage, and target binding kinetics. The analysis window was set manually onto 1 min after sample injection in order to prevent the mechanical disturbance caused by emptying and refilling the microfluidic chambers from affecting the calculations. The integrated impedance signal response (integrated area) was calculated as the area under the binding curve starting at the point of sample injection and ending at 1200 s.

RESULTS AND DISCUSSION

The objective of our investigation was to explore the feasibility of employing an antimicrobial peptide from class IIa bacteriocins in an impedance analyzer for selective and sensitive detection of harmful microorganisms and, in particular, *L. monocytogenes*. Optimum impedance frequency range for the detection was determined by exposing the peptide sensor to various samples with and without target cells at different frequencies (10−120 Hz). Figure 2A illustrates the optimum frequency for using the AMP designed sensor in detecting spoilage bacterial species. Although all the investigated frequencies exhibited clear impedimetric responses to bacterial cells, 100 Hz appeared to be the optimum frequency within the constraints of our experimental setup.

Sensitivity. The sensitivity of microbial detection is a very critical parameter in determining the practical applicability of the functionalized sensor.[13,39] To this end, the sensitivity of the LeuA-functionalized sensor (peptide sensor) in detecting microbial cells was probed by exposing the sensor to various concentrations of bacteria. Figure 2B shows the results of measurements performed after incubation of the peptide sensor with pathogenic *L. monocytogenes* in concentrations ranging from 10^2 to 10^6 cfu mL^{-1}. A "control sensor" with cysteamine-functionalized microelectrode array treated with the same concentrations of bacteria and a "blank" peptide sensor treated with target-free (no bacteria) samples were also subjected to impedance readings for comparisons. The results revealed that variation in the impedance signal response is directly proportional to the number of bacterial cells bound to the peptide sensor (LeuA-immobilized array) and that variation is expressed in a logarithmic increase with respect to serially diluted bacterial cells. The lowest limit of detection of this peptide microelectrode device to *L. monocytogenes* was found to be 10^3 cfu mL^{-1}, i.e., 1 bacterium/μL, which is a clinically significant value,[40] and it compares well with other detection assays such as antibody-based impedance and AMP-based fluorescence tests.[17,41]

In order to simulate the applicability of this peptide sensor in everyday applications and in on-site detection, the detection was performed in a real time, without any extrinsic labels. The dynamic parameters of the peptide−bacteria interactions were

dx.doi.org/10.1021/ac4034938 | Anal. Chem. 2014, 86, 1693−1700

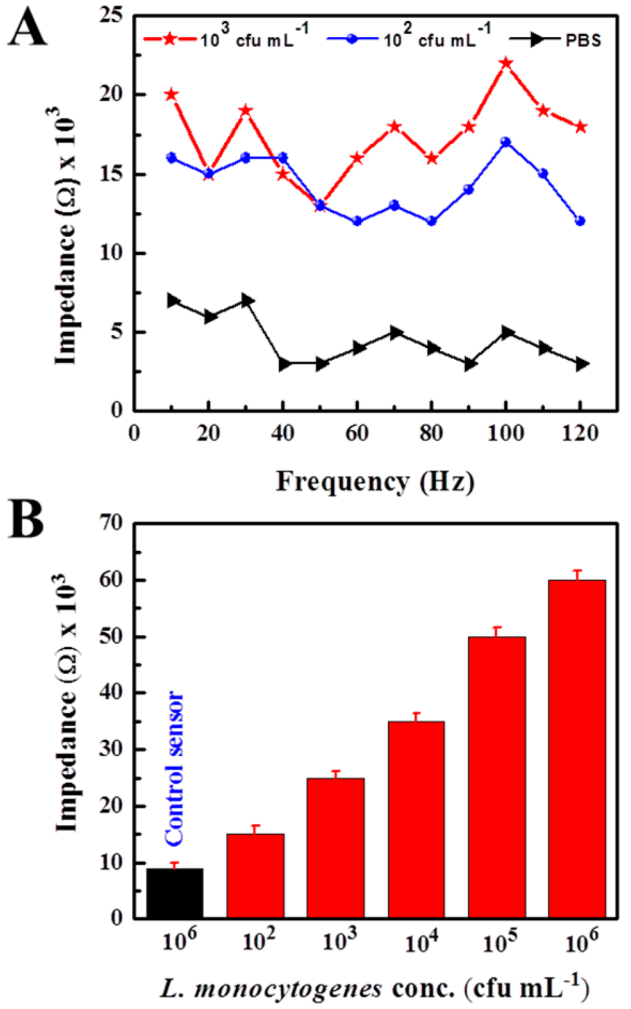

Figure 2. (A) Impedance spectra of the peptide sensor response to *L. monocytogenes* (red) and *E. faecalis* (blue) at concentrations of 10^3 cfu mL^{-1} as well as its response to a PBS solution (black) at multiple frequencies. (B) Impedance spectra of the peptide sensor response to various concentrations of *L. monocytogenes* at a fixed frequency (100 Hz). A control sensor (cysteamine-functionalized sensor) was used for comparison. Error bars show the standard deviations.

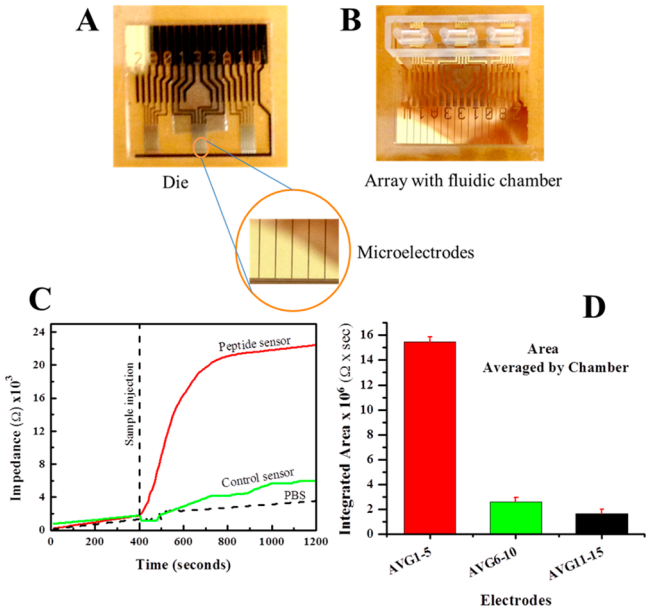

Figure 3. Real-time measurements of binding of bacteria to the peptide sensor. Panel A shows the die or impedimetric sensor microarray with the interdigitated gold microelectrodes, whereas panel B shows a photograph of the impedance array attached to a microfluidic chamber. (C) Binding curves for the normalized impedance signals from specific binding of *L. monocytogenes* (10^3 cfu mL^{-1}) to a peptide sensor (red line) and a control sensor (green line). The peptide sensor response to PBS was used as a blank (black dashed line). (D) The binding curve parameter (integrated area under the curve) for the response to *L. monocytogenes* binding to the peptide sensor (red), control sensor (green), and response of PBS binding to the peptide sensor (black). Each impedance response and calculated area are an average calculation of five replicates; error bars indicate corresponding standard deviations.

further estimated accordingly. As shown in Figure 3, impedance microelectrodes (Figure 3A) were first functionalized with LeuA as described in the Materials and Methods section. A microfluidic chamber with three separate cells was then attached to the functionalized microelectrodes, where each cell is hosting five microelectrodes (Figure 3B). The fluidic chambers were initially filled with buffer solution (target-free sample, without bacteria) and subjected to impedance reading for 400 s to determine the baseline. Subsequently, *L. monocytogenes* solution (20 μL, 10^3 cfu mL^{-1}) was incubated with the functionalized microelectrodes and the impedance was measured for 800 s. The impedance response was continuously monitored before and after injection of the bacterial samples. As it is seen in Figure 3C, the peptide sensor produces a measurable response to bacterial sample relative to the blank and the control sensors. A clear signal and strong response starts immediately after sample injection, indicating adhesion of the bacterial cells to the immobilized peptide on the sensor surface. The impedance shows large changes that are clearly attributed to the binding of the immobilized AMP to the target bacterial cells. The results are in agreement with a similar study done by Mannoor et al.,[18] where they revealed that peptide microcapacitive hybrid impedance was able to demonstrate both Gram-selective detection and interbacterial strain differentiation, while maintaining recognition capabilities toward pathogenic strains of *E. coli* and *Salmonella*.[18] The same study was also able to reveal a detection limit of approximately 1 bacterium/μL.[18]

Further insight on the selectivity of the immobilized AMP toward *L. monocytogenes* was achieved by analyzing the kinetic parameters of the peptide−bacteria interactions. The integrated area under the binding curve was algorithmically calculated for each sensor, and a representative graph is plotted in Figure 3D. Clearly, the integrated areas show a strong correlation between specific binding of the peptide sensor to *L. monocytogenes* and the physical adsorption to the control sensors.

Selectivity. We investigated the selectivity in binding of the AMP-functionalized sensor toward various bacterial species and determined the binding kinetics of each strain. In particular, binding affinity of the peptide sensor was explored against four Gram-positive strains, namely, *L. monocytogenes*, *L. innocua*, *E. faecalis*, and *S. aureus*. In a previous study, we have shown the capability of surface immobilized with a short segment of class IIa bacteriocin (LeuA) to bind selectively to Gram-positive strains at high concentrations using fluorescence microscopy methods.[23] The method, however, did not demonstrate high sensitivity, nor did it show capability for label-free multiplexed detection of different strains in real time.[23] This study on the

dx.doi.org/10.1021/ac4034938 | *Anal. Chem.* 2014, 86, 1693−1700

other hand demonstrates that combining the antimicrobial peptide with the impedance spectroscopy allows discrimination between various bacterial species at a concentration of 10^3 cfu mL^{-1}. Figure 4A reveals a real-time impedimetric response of

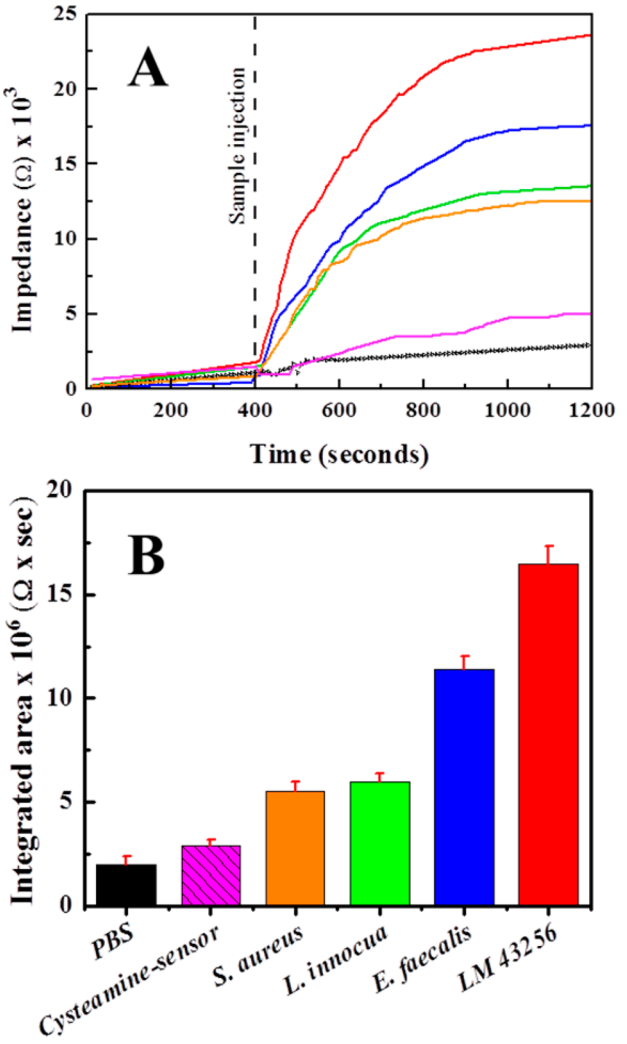

Figure 4. (A) Real-time impedimetric response of the peptide sensor to various bacterial species (10^3 cfu mL^{-1}) at 100 Hz. The red, blue, green, and orange signals correspond to the peptide sensor response to *L. monocytogenes* (LM 43256), *E. faecalis*, *L. innocua*, and *S. aureus*, respectively. The pink-colored signal is the control sensor response to *L. monocytogenes*, and the dashed black line is the peptide sensor signal against the PBS solution. (B) The binding curve parameter (integrated area under the curve) for impedance sensor responses to the corresponding strains. Note that each impedance response is an average calculation of five replicates and error bars indicate corresponding standard deviations.

the peptide sensor to various bacterial species at 100 Hz. The red signal corresponds to peptide sensor response to *L. monocytogenes*, while the blue, green, and orange represent the peptide sensor interactions for *E. faecalis*, *L. innocua*, and *S. aureus*, respectively. The peptide sensor clearly displays the highest impedimetric signal response against *L. monocytogenes*, where the amplitude is increased from 500 Ω at the baseline to reach ~2.4×10^4 Ω. The next uppermost impedance signal was observed for *E. faecalis*, where impedance shifted to nearly 1.8×10^4 Ω from its starting point after the sample injection. Finally, impedance reached 1.43×10^4 and 1.35×10^4 Ω due to peptide sensor responses to both *L. innocua* and *S. aureus*, respectively. The variation in the impedimetric responses between bacterial strains is attributed to a number of potential factors. For instance, differential expression level of the man-PTS receptors on the surface of the target cells from one strain to another would give rise to different binding sensitivity of the immobilized AMP to bacterial strains, which thereby lead to distinctive impedance sensor responses. Indeed, few studies have recently shown that number of the molecular receptors at the cellular membrane of the bacterial cells play crucial role in peptide–bacteria interactions and that biological activity of the AMP depends on the level of the expressed receptors at the bacterial cell membrane.[32,33,42] Likewise, Kjos et al. showed that the level of bacteriocin susceptibility of the bacterial cell was predominantly dictated by differences in expression of man-PTS proteins and that bacteriocin sensitivity can vary within the same species, due to differential expression levels of the same man-PTS receptor.[32] Class IIa bacteriocins bind the man-PTS receptor; therefore, these AMPs can be used mainly for detecting Gram-positive strains that express man-PTS on their surface. Class IIa bacteriocins are inactive against Gram-negative bacteria, and man-PTSs are not found in eukaryotes; therefore, these peptides are highly specific for Gram-positive strains. However, this class of AMPs may not differentiate between strains that express same number and type of man-PTS receptors.

The algorithm[38] we used allowed obtaining further insight of the peptide–bacteria interactions by extracting the kinetic parameters of the peptide sensor responses to bacterial species. The integrated areas under the binding curve of each strain that interacts with the immobilized AMP were calculated and graphically plotted in Figure 4B. In agreement with the real-time measurements, the integrated areas showed that the highest area accounted for peptide sensor response to binding of *L. monocytogenes* to the immobilized AMP.

For a comparative quantification of binding of the different species to the peptide sensor, the parameters A, s, and $A \times s$ were algorithmically calculated for the different bacterial species (Supporting Information Figure S1). The intended parameters revealed the target concentration, sensor surface coverage, as well as the binding kinetics. While the amplitude A is proportional with the sensor surface converge of the target cells and indicative to the affinity of the analytes–receptor interactions, the time constant (s value) is relative to the binding rate constant, which is in fact independent of the amplitude A. The $A \times s$ value represents the initial rate of binding. We can infer that a combination of both parameters A and s provided a signature of the binding event and allowed one to obtain further comprehensive characteristic of peptide–target binding behavior.

Real-Time Detection in Milk Samples. In order to investigate the applicability of the present AMP-based sensor array in real-life applications, we have used it for detection of bacteria in artificially contaminated milk sample. First, we optimized the milk concentration for the impedimetric detection. Unlike the PBS, the milk has a very high molecular density due to its components from fats, sugars, enzymes, and proteins. Those components, unfortunately, could cross-react and interfere with the target cells in the detection and lead to false positive or negative results.[43] For these reasons, a concentration of 10^3 cfu mL^{-1} of *L. monocytogenes* was artificially incubated with a number of serially diluted milk samples ranging from 10% to 100% in PBS solution. An aliquot

dx.doi.org/10.1021/ac4034938 | *Anal. Chem.* 2014, 86, 1693–1700

(20 μL) from each sample was incubated with the AMP-fabricated microelectrodes in the impedance microfluidic chamber, and the impedance measurements were carried out for 800 s at 100 Hz. The optimization of the assay was performed through the analysis of the amplitude of specific binding versus nonspecific (controls) signals (Figure 5A). The

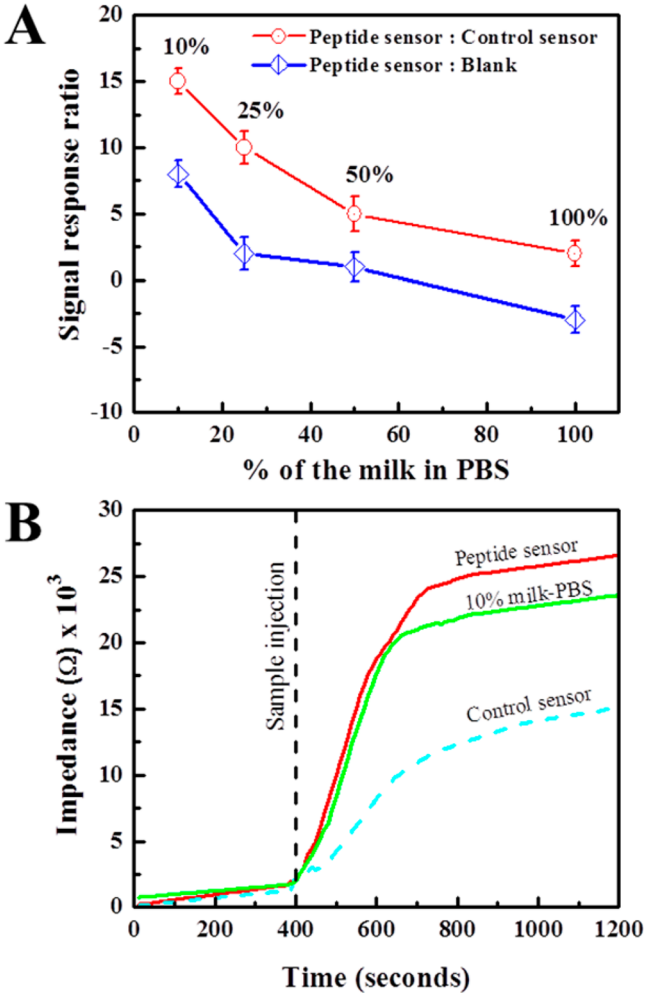

Figure 5. (A) Signal response ratios of specific targets (peptide–bacteria) vs controls (cysteamine–bacteria and peptide–PBS). The red curve corresponds to the ratio of amplitude of peptide–bacteria interaction (peptide sensor) and cysteamine–bacteria (control sensor) interaction, whereas the blue signal correlates to the ratio of amplitude of peptide–bacteria interaction (peptide sensor) and peptide–PBS (blank) interaction. Ratios were calculated at different milk concentrations (10–100% milk in PBS). (B) Real-time label-free detection of *L. monocytogenes* (10^3 cfu mL^{-1}) in 10% milk at 100 Hz. Impedance response was recorded for the peptide sensor when exposed to contaminated milk (red) or pure milk (green, no bacteria), as well as for the control sensor (cysteamine) when exposed to contaminated milk (dashed cyan). Each impedance response is an average calculation of five replicates, and error bars indicate corresponding standard deviations.

calculated ratio of specific and nonspecific signal amplitude shows an optimum at 10% milk in PBS (1:9). In contrast, plain milk with 100% concentration shows a very different pattern and depraved signal response indicating interference. Milk proteins and fats beside other components seem to interact nonspecifically with the peptide sensor and lead to strong impedance changes. In fact, it has been previously shown that milk components nonspecifically interact with the impedance response of the interdigitated electrodes giving rise to an increase in the resistance.[43−45] Furthermore, high density of fats and proteins could raise the possibility of peptide–protein and/or peptide–lipid interactions that could lead to false positive results.[46,47]

Figure 5B depicts a real-time label-free detection of *L. monocytogenes* (10^3 cfu mL^{-1}) in 10% milk sample at 100 Hz. The curves showed sufficient resolution on impedance responses between milk and contaminated milk. Also, the control sensor displayed much less response compared to the peptide sensor when subjected to contaminated milk sample. Analysis of the binding curve parameters, such as integrated area (Supporting Information Figure S2A), amplitude A (Supporting Information Figure S2B), time constant s (Supporting Information Figure S2C) as well as the initial rate of binding $A \times s$ (Supporting Information Figure S2D), revealed further substantial resolutions with approximately 3–4-fold difference between the peptide senor responses to bacterial samples and the controls. The experiment establishes that the sensor responses show significant nonspecific adsorption of the fats, proteins, and carbohydrates present in the milk with no clear detection of bacteria at high density of the milk. On the other hand, at a concentration of 10% milk/PBS, the peptide sensor was able to provide excellent specific/nonspecific resolution and detect *L. monocytogenes* at very low level of concentration.

Sensor Array Regeneration. The microelectrode array was regenerated through vigorously washing the microfluidic chamber with 70% ethanol solution in order to completely remove all adhered bacterial cells and making the functionalized array accessible for the next detection process. The array performance after regeneration was evaluated against *L. monocytogenes* at a concentration of 10^3 cfu mL^{-1} in 1× PBS solution at a fixed frequency. Supporting Information Figure S3 shows the dependence of assay parameters A, s, and $A \times s$ on the number of array reuses. The amplitude A declined rapidly after the third reuse to approximately 50% of the initial value. The time constant and the initial binding have also changed erratically from the first time use. It may be that the excessive use of ethanol for washing the cells from the sensor surface damaged the sensor array electrical properties and led to improper integration of the results. These results suggest that the steps for regeneration of the peptide-immobilized microelectrode array need optimization. Milder conditions such as use of 40% ethanol twice could preserve array performance.

Owing to the selective nature of the interaction of class IIa bacteriocins with pathogenic bacteria, specifically *L. monocytogenes*,[24,48] the discrimination of multiple species of pathogenic Gram-positive bacteria has been achieved in buffer solutions. However, it has been very challenging to detect bacteria in pure milk samples. Future work will focus on obtaining a well-defined discrimination pattern between bacterial species in milk samples and other food products. The approach will involve exploring different strategies to improve sensitivity and selectivity via employing alternative techniques for covalent immobilization of the AMPs, investigating multiligands, and using other sensor platforms in parallel to achieve better detection limit with relevant selectivity using a multimodal approach.

dx.doi.org/10.1021/ac4034938 | *Anal. Chem.* 2014, 86, 1693−1700

CONCLUSION

An impedimetric biosensor platform for bioaffinity assay was developed based on a real-time, label-free detection using antimicrobial peptide from class IIa bacteriocins. The biosensor was capable of distinguishing between closely related bacterial strains and was able to detect very low concentration of *L. monocytogenes* with limits of detection as low as 10^3 cfu mL^{-1}, or 1 bacterium/μL—a clinically relevant limit. The data analysis algorithm extracted multiple parameters of binding curve kinetics, all of which were essential for analysis of target–peptide interactions in real time. This fully integrated AMP-based sensor array can be potentially used for detection of a wide range of analytes of practical significance and has the prospective of use as a robust, portable biosensor device to efficiently detect pathogenic strains in food samples.

ASSOCIATED CONTENT

Supporting Information

Figures S1–S3 related to binding curve parameters of normalized impedance signal responses. This material is available free of charge via the Internet at http://pubs.acs.org.

AUTHOR INFORMATION

Corresponding Author

*Phone: 780-492-8917. Fax: 780-492-1217. E-mail: kkaur@ualberta.ca.

Notes

The authors declare no competing financial interest.

ACKNOWLEDGMENTS

We acknowledge the Natural Sciences and Engineering Research Council of Canada (NSERC) for supporting this research. We also thank Michelle Stiles, Denise Carlson, and Sushanta Mitra for in-depth discussion and illustrations. H. Etayash is the recipient of a Ph.D. scholarship under the Libyan–North American Scholarship Program.

REFERENCES

(1) Farahi, R. H.; Passian, A.; Tetard, L.; Thundat, T. *ACS Nano* **2012**, *6*, 4548–4556.
(2) Donnenberg, M. S.; Narayanan, S. *Infect. Dis. Clin. North Am.* **2013**, *27*, 535–554.
(3) Gracias, K. S.; McKillip, J. L. *Can. J. Microbiol.* **2004**, *50*, 883–890.
(4) Rasooly, A.; Herold, K. E. *J. AOAC Int.* **2006**, *89*, 873–883.
(5) Beyor, N.; Yi, L.; Seo, T. S.; Mathies, R. A. *Anal. Chem.* **2009**, *81*, 3523–3528.
(6) Li, Y.; Cu, Y. T.; Luo, D. *Nat. Biotechnol.* **2005**, *23*, 885–889.
(7) Johnson, R. P.; Durham, R. J.; Johnson, S. T.; MacDonald, L. A.; Jeffrey, S. R.; Butman, B. T. *Appl. Environ. Microbiol.* **1995**, *61*, 386–388.
(8) Daly, P.; Collier, T.; Doyle, S. *Lett. Appl. Microbiol.* **2002**, *34*, 222–226.
(9) Soleymani, L.; Fang, Z.; Sargent, E. H.; Kelley, S. O. *Nat. Nanotechnol.* **2009**, *4*, 844–848.
(10) Sorgenfrei, S.; Chiu, C. Y.; Gonzalez, R. L., Jr.; Yu, Y. J.; Kim, P.; Nuckolls, C.; Shepard, K. L. *Nat. Nanotechnol.* **2011**, *6*, 126–132.
(11) Slinker, J. D.; Muren, N. B.; Gorodetsky, A. A.; Barton, J. K. *J. Am. Chem. Soc.* **2010**, *132*, 2769–2774.
(12) Nilsson, K. G.; Mandenius, C. F. *Biotechnology* **1994**, *12*, 1376–1378.
(13) Arora, P.; Sindhu, A.; Dilbaghi, N.; Chaudhury, A. *Biosens. Bioelectron.* **2011**, *28*, 1–12.
(14) Bergwerff, A. A.; van Knapen, F. *J. AOAC Int.* **2006**, *89*, 826–831.
(15) Swaminathan, B.; Feng, P. *Annu. Rev. Microbiol.* **1994**, *48*, 401–426.
(16) Zasloff, M. *Nature* **2002**, *415*, 389–395.
(17) Kulagina, N. V.; Lassman, M. E.; Ligler, F. S.; Taitt, C. R. *Anal. Chem.* **2005**, *77*, 6504–6508.
(18) Mannoor, M. S.; Zhang, S.; Link, A. J.; McAlpine, M. C. *Proc. Natl. Acad. Sci. U.S.A.* **2010**, *107*, 19207–19212.
(19) McAlpine, M. C.; Agnew, H. D.; Rohde, R. D.; Blanco, M.; Ahmad, H.; Stuparu, A. D.; Goddard, W. A., III; Heath, J. R. *J. Am. Chem. Soc.* **2008**, *130*, 9583–9589.
(20) Cui, Y.; Kim, S. N.; Naik, R. R.; McAlpine, M. C. *Acc. Chem. Res.* **2012**, *45*, 696–704.
(21) Yang, L.; Bashir, R. *Biotechnol. Adv.* **2008**, *26*, 135–150.
(22) Mannoor, M. S.; Tao, H.; Clayton, J. D.; Sengupta, A.; Kaplan, D. L.; Naik, R. R.; Verma, N.; Omenetto, F. G.; McAlpine, M. C. *Nat. Commun.* **2012**, *3*, 763.
(23) Etayash, H.; Norman, L.; Thundat, T.; Kaur, K. *Langmuir* **2013**, *29*, 4048–4056.
(24) Cotter, P. D.; Hill, C.; Ross, R. P. *Nat. Rev. Microbiol.* **2005**, *3*, 777–788.
(25) Vagin, M. Y.; Trashin, S. A.; Karyakin, A. A.; Mascini, M. *Anal. Chem.* **2008**, *80*, 1336–1340.
(26) Hu, Y.; Zuo, P.; Ye, B. C. *Biosens. Bioelectron.* **2013**, *43*, 79–83.
(27) Chung, Y. K.; Reboud, J.; Lee, K. C.; Lim, H. M.; Lim, P. Y.; Wang, K. Y.; Tang, K. C.; Ji, H.; Chen, Y. *Biosens. Bioelectron.* **2011**, *26*, 2520–2526.
(28) Cotter, P. D.; Ross, R. P.; Hill, C. *Nat. Rev. Microbiol.* **2013**, *11*, 95–105.
(29) Drider, D.; Fimland, G.; Hechard, Y.; McMullen, L. M.; Prevost, H. *Microbiol. Mol. Biol. Rev.* **2006**, *70*, 564–582.
(30) Kaur, K.; Andrew, L. C.; Wishart, D. S.; Vederas, J. C. *Biochemistry* **2004**, *43*, 9009–9020.
(31) Jacquet, T.; Cailliez-Grimal, C.; Francius, G.; Borges, F.; Imran, M.; Duval, J. F.; Revol-Junelles, A. M. *Res. Microbiol.* **2012**, *163*, 323–331.
(32) Kjos, M.; Nes, I. F.; Diep, D. B. *Microbiology* **2009**, *155*, 2949–2961.
(33) Ramnath, M.; Arous, S.; Gravesen, A.; Hastings, J. W.; Hechard, Y. *Microbiology* **2004**, *150*, 2663–2668.
(34) Wang, Y.; Henz, M. E.; Gallagher, N. L.; Chai, S.; Gibbs, A. C.; Yan, L. Z.; Stiles, M. E.; Wishart, D. S.; Vederas, J. C. *Biochemistry* **1999**, *38*, 15438–15447.
(35) Bodapati, K. C.; Soudy, R.; Etayash, H.; Stiles, M.; Kaur, K. *Bioorg. Med. Chem.* **2013**, *21*, 3715–3722.
(36) Costa, F.; Carvalho, I. F.; Montelaro, R. C.; Gomes, P.; Martins, M. C. *Acta Biomater.* **2011**, *7*, 1431–1440.
(37) Ghindilis, A. L.; Smith, M. W.; Messing, D. S.; Haynes, V. N.; Middleton, G. B.; Schwarzkopf, K. R.; Campbell, C. E.; Zhan, C.; Ulrich, B.; Frasier, M. J.; Schuele, P. J.; Evans, D. R.; Sezan, I.; Hartzell, J. W.; Simon, H. M. *Biosens. Bioelectron.* **2012**, *35*, 87–93.
(38) Messing, D. S.; Ghindilis, A.; Schwarzkopf, K. *Conf. Proc. IEEE Eng. Med. Biol. Soc.* **2011**, *2011*, 2740–2744.
(39) Sensors, Safety and SPR. *Nature* **2000**, *403*, 343–344
(40) Li, Y.; Karlin, A.; Loike, J. D.; Silverstein, S. C. *Proc. Natl. Acad. Sci. U.S.A.* **2002**, *99*, 8289–8294.
(41) Barreiros dos Santos, M.; Agusil, J. P.; Prieto-Simon, B.; Sporer, C.; Teixeira, V.; Samitier, J. *Biosens. Bioelectron.* **2013**, *45*, 174–180.
(42) Kjos, M.; Borrero, J.; Opsata, M.; Birri, D. J.; Holo, H.; Cintas, L. M.; Snipen, L.; Hernandez, P. E.; Nes, I. F.; Diep, D. B. *Microbiology* **2011**, *157*, 3256–3267.
(43) Liebana, S.; Lermo, A.; Campoy, S.; Cortes, M. P.; Alegret, S.; Pividori, M. I. *Biosens. Bioelectron.* **2009**, *25*, 510–513.
(44) Dapra, J.; Lauridsen, L. H.; Nielsen, A. T.; Rozlosnik, N. *Biosens. Bioelectron.* **2013**, *43*, 315–320.
(45) Fernandez, F.; Hegnerova, K.; Piliarik, M.; Sanchez-Baeza, F.; Homola, J.; Marco, M. P. *Biosens. Bioelectron.* **2010**, *26*, 1231–1238.
(46) Causey, L. D.; Dwyer, D. S. *Nat. Biotechnol.* **1996**, *14*, 348–351.

(47) Zhang, Z.; Zhu, W.; Kodadek, T. *Nat. Biotechnol.* **2000**, *18*, 71−74.
(48) Diep, D. B.; Skaugen, M.; Salehian, Z.; Holo, H.; Nes, I. F. *Proc. Natl. Acad. Sci. U.S.A.* **2007**, *104*, 2384−2389.

NOTE ADDED AFTER ASAP PUBLICATION

Due to a production error, this paper was published on the Web on January 21, 2014, with several references cited incorrectly. The corrected version was reposted on January 22, 2014.